Proceedings World Geothermal Congress 2000
Kyushu - Tohoku, Japan, May 28 - June 10, 2000

VELOCITY STRUCTURES OF KAKKONDA AREA ESTIMATED BY 3-D SIMULATIONS

Tsuneo Kikuchi[1] and Yuji Nishi[1]

[1]Geological Survey of Japan, 1-1-3, Higashi, Tsukuba, Japan

Key Words: geophysical techniques, velocity structure, simulation

ABSTRACT

The purpose of this paper is to clarify the velocity structures within the Kakkonda geothermal field, northern Japan. For this purpose, 3-D numerical simulations, using the staggered grid finite-difference method, were carried out. To verify simulation programs, we adopted a model consisting of two layers: velocities of P and S wave were 3600 m/s and 2144 m/s for the first layer, and 4272 m/s and 2415 m/s for the second layer respectively, at a grid interval of 10 m. This model covered an area of 1.6 (N-S) x 1.6 (E-W) km^2 at a depth of 1.8 km. The dominant frequency of the source was assumed to be 4 Hz. Calculated P wave first arrivals agreed well with theoretical values for this model. Consequently, a four layer model, for which the dominant frequency of the source was higher and the grid interval smaller (=5 m), was calculated. Therefore, the errors between observed first arrivals of P waves and those calculated were ±1% within the model where the velocities of P and S wave were about 20 % larger than the 1-D inversion model and a partial low velocity zone existed.

1. INTRODUCTION

Fracture network systems play an important role in geothermal reservoirs. Microearthquake surveys are one of the most useful methods used to detect fracture networks as part of the seismic activity is related to fluid flow through fractures. An exact 3-D velocity structure is essential for estimating seismic sources correctly.

The New Energy and Industrial Technology Development Organization (NEDO) and the Japan Metals and Chemicals Co. carried out an investigation, using explosives, for the estimation of the velocity structure of Kakkonda area in 1993. The survey was made using dynamite, in well KT-208, at five depths: 900, 800, 700, 600 and 500 m. We observed waveforms with a small array of five seismographs (L-4C, the effective instrumental period is 1 s) which were set 700 m northwest of well KT-208. We then compared the observed waveforms with those calculated from numerical simulations (Kikuchi and Nishi, 1997). For this analysis, we used two waveforms recorded at two observation points (TA-31 and TA-36) because the data quality of these points was fairly good. We adopted a staggered grid finite-difference algorithm (Virieux, 1984, 1986) to model the Kakkonda area. The model used for the simulation was two-dimensional and was based on the 1-D inversion analysis of the velocity structure (NEDO, 1996). The dimensions of this model were 2 km in width by 2 km in depth, with the origin at well KT-208. Velocities of P and S waves in this model were 2819 m/s and 1208 m/s for the first layer; 3960 m/s and 2358 m/s for the second layer; 4272 m/s and 2415 m/s for third layer; and 4678 m/s and 2686 m/s for fourth layer, respectively. The errors between observed first arrivals of P waves and those calculated were ±5%.

The Kakkonda area is topographically irregular, especially to the northeast to southwest, which is perpendicular to the simulation model described above. Therefore, we calculated wave propagation using a three-dimensional model to estimate the effects of topography. Calculations of wave propagation using 3-D models are difficult because of limitations of computer capabilities - principally memory restrictions. To overcome these problems, we developed a parallel-processing program for calculating the wave propagation of the 3-D model. Calculating the 3-D wave propagation of Kakkonda area using the parallel-processing program is an original approach.

For this project, we first calculated wave propagation, using a 3-D model consisting of two layers, for verification of the simulation programs. The grid spacing of this model was 10 m. Calculated P wave first arrivals agreed well with theoretical values. Second, we used the same four-layered model with the grid spacing reduced to 5 m and a source center frequency of 6.7 Hz. The errors between observed first arrivals of P waves and those calculated were ±1% within the model where the velocities of P and S wave were about 20 % larger than the 1-D inversion model (NEDO, 1996) and where a partial low velocity zone exists.

2. METHOD

Standard finite-differencing techniques are not stable for models with large contrasts in Poisson's ratio, such as found at fluid-solid or solid-gas contacts. However, the staggered grid finite-difference method overcomes the stability problem (Yoon and McMechan, 1992) by allowing for complex structures including the surface of the earth. The size of the simulation model is mainly limited by computer memory. Therefore, reflections from edges of the model usually occur. These reflections are artificial, so we adopted an absorbing boundary to prevent these reflections (Sochacki et al., 1987).

3. MODEL

First, we verified the simulation programs by calculating wave propagation using a 3-D model consisting of two layers. The model dimensions were 1.6 km by 1.6 km by 1.8 km, the grid spacing was 10 m, and the dominant frequency of the source was 4 Hz. The elevation ranged from 1450 m to -350 m. Velocities of P and S waves were 3600 m/s and 2144 m/s for the first layer and 4272 m/s and 2415 m/s for the second layer, respectively. The elevation of the first layer was 350 m. The P and S wave velocities were estimated using 1-D velocity inversion analysis (NEDO, 1996). A low velocity zone above 789 m in elevation (velocities of 2563 m/s and 1098 m/s) was expected. However, this low velocity zone was thin in our simulation model and we disregarded it to simplify calculations. We used a digital 50 m grid map published by Geographical Survey Institute to generate 10 m grid of the surface of Kakkonda field. The position of the source was the center of the model and was 800 m from the surface (-120 m a.s.l.). The pressure source was defined on a " six point star" centered at this depth (Yoon and McMechan, 1992). In this calculation, the time step Δt was 1.2 ms and the number of steps was 1200, so the total calculated time was 1.44 s. Calculated P wave first arrivals at the surface, near well KT-208, agreed with theoretical values and also agreed with the observed values from the explosive investigation. Therefore, we concluded that the programs for 3-D simulation function satisfactorily.

Second, we calculated wave propagation using the full four-layered model with grid spacing reduced to 5 m and a source center frequency of 6.7 Hz. Dimensions of this model were 2.0 km by 2.0 km by 2.0 km. Fig. 1 shows the surface of this model. Well KT-208, shown by the black circle, was chosen as the coordinate origin. Five seismographs are shown by symbols + and the positions of TA-31 and TA-36 are shown by arrows. Fig. 2 shows the waveform of the source used in simulations and its Fourier amplitude spectrum. The position of the source was the same as the small model. In this calculation, time step Δt was 0.4 ms, the number of steps was 1250, and the total calculated time was 0.5 s. Table 1 shows the model parameters. P and S velocities are same as the 2-D model.

For these calculations, we used several different computers such as the CRAY C90, DEC cluster, IBM RS/6000-SP, and SR8000 of Tsukuba Advanced Computing Center.

4. RESULTS

Fig. 3 shows the seismograms of the 800 m explosion. Fig. 3(a) shows TA-31 and Fig 3(b) shows TA-36. The top line shows the observed record, the middle line shows the 2-D, and the bottom line shows the 3-D calculated seismogram. The horizontal axis is time and the vertical axis is amplitude normalized by the maximum amplitude of each waveform. P wave first arrivals are also shown. The source frequency of 2-D calculation is 15 Hz - which is higher than the 3-D calculation.

However, no difference existed between P wave first arrivals of 2-D and 3-D calculations in spite of waveform differences. Observed P wave first arrivals of TA-31 and TA-36 were 2 ms and 14 ms faster than calculated P wave first arrivals respectively. Therefore, we calculated wave propagation for a new model. This model's P and S velocities were 3076 km/s and 1318 for the first layer and 4272 m/s and 2415 m/s for the second and third layers respectively. The velocities of the fourth layer were the same as those used in the old model.

Fig. 4 shows the seismograms of this model for the 800 m explosion. Fig. 4(a) shows TA-31. Fig 4(b) shows TA-36. The top lines show the observed record and the bottom lines show the 3-D calculated seismogram. The two axes are the same as Fig. 3. In this model the observed P wave first arrival for TA-31 is 9 ms later than calculated P wave first arrival. The observed and calculated P wave first arrival for TA-36 were almost same.

5. DISCUSSION

To minimize the difference between observed and calculated P wave first arrivals for TA-31, we assumed a model where a low velocity zone existed around TA-31. The width of this zone was 25 m. Velocities of P and S waves for this zone are 1282 m/s and 549 m/s respectively. Fig. 5 shows the seismograms of this model for the 800 m explosion. The observed P wave first arrival for TA-31 was only 3 ms faster than calculated P wave first arrival. Errors between observed and calculated P first arrivals for TA-31, TA-36 are 1.0 and 0.7 %, respectively.

6. CONCLUSIONS

We have developed a parallel 3-D simulation program using a staggered-grid finite-difference algorithm and have tested it against standard models. Using this program, we calculated wave propagation for a four-layered model of Kakkonda field including complex surface topography. In this calculation, the differences between observed and calculated P wave first arrivals were minimum for the model where velocities of P and S waves are 3076 m/s and 1318 m/s for the first layer; 4272 m/s and 2415 m/s for the second and third layers; and 4768 m/s and 2686 m/s for the fourth layer respectively, and a low velocity zone exists around TA-31.

7. REFERENCES

Kikuchi, T., and Nishi, Y. (1997). Velocity structures of Kakkonda area estimated by simulations. *1997 Annual meeting geothermal research society of Japan abstracts with programs*.

NEDO, 1996, *Report for study on geothermal resources exploration techniques, deep-seated geothermal resource survey*.

Sochacki, J., Kubichek, R., George, J., Fletcher, W. R., and Smithson, S. (1987). Absorbing boundary conditions and surface waves. *Geophysics*, Vol. 52(1), pp. 60-71.

Virieux, J. (1984). SH-wave propagation in heterogeneous media: Velocity-stress finite-difference method. *Geophysics*, Vol. 49(11), pp. 1933-1942.

Virieux, J. (1986). P-SV wave propagation in heterogeneous media: Velocity-stress finite-difference method. *Geophysics*, Vol. 51(4), pp. 889-901.

Yoon, K. -H., and McMechan, G. A. (1992) 3-D finite-difference modeling of elastic waves in borehole environments. *Geophysics*, Vol. 57(6), pp. 793-804.

Table 1 Model parameters.

Layer	1	2	3	4
P wave velocity(m/s)	2819	3960	4272	4768
S wave velocity(m/s)	1208	2358	2415	2686
Density(kg/m^3)	2206	2401	2506	2576
Depth(m)	>789	789-350	350--235	<-235

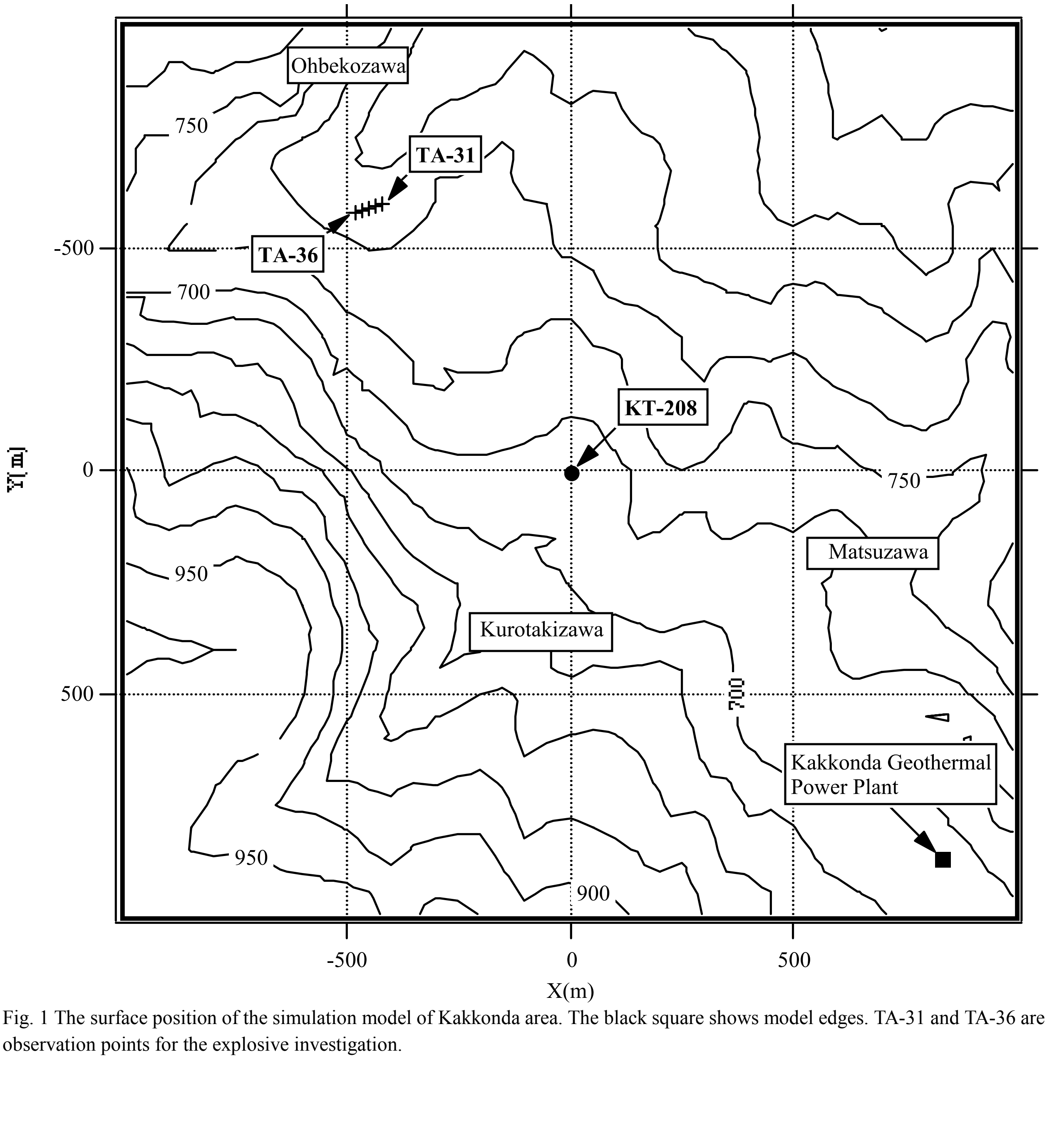

Fig. 1 The surface position of the simulation model of Kakkonda area. The black square shows model edges. TA-31 and TA-36 are GSJ's observation points for the explosive investigation.

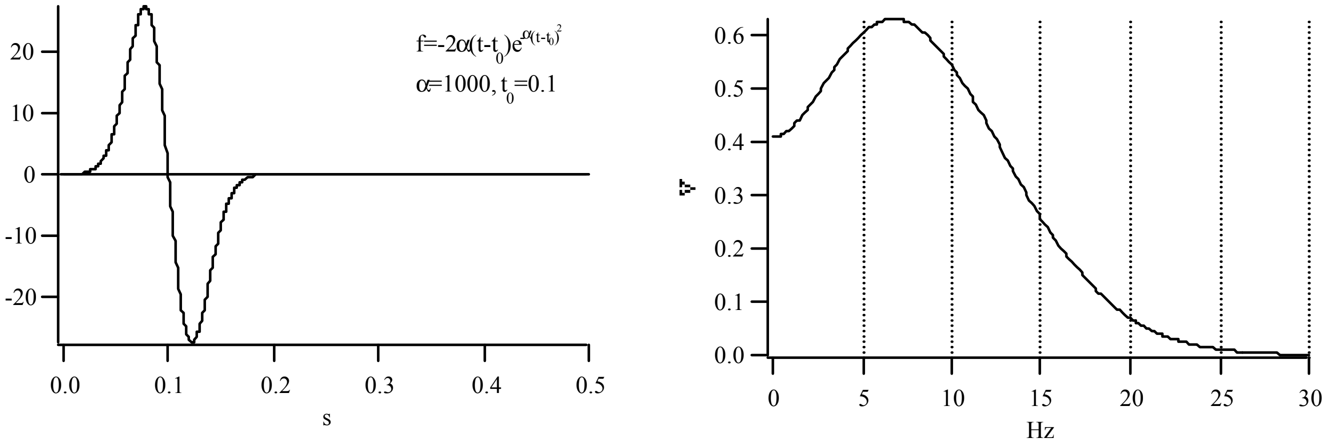

Fig. 2 The waveform of the source used in simulations and its Fourier amplitude spectrum.

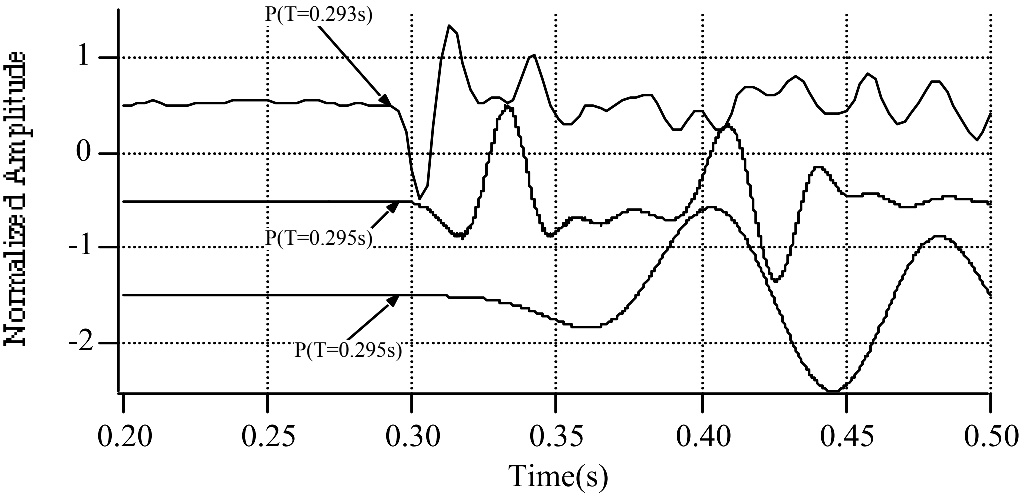

(a)

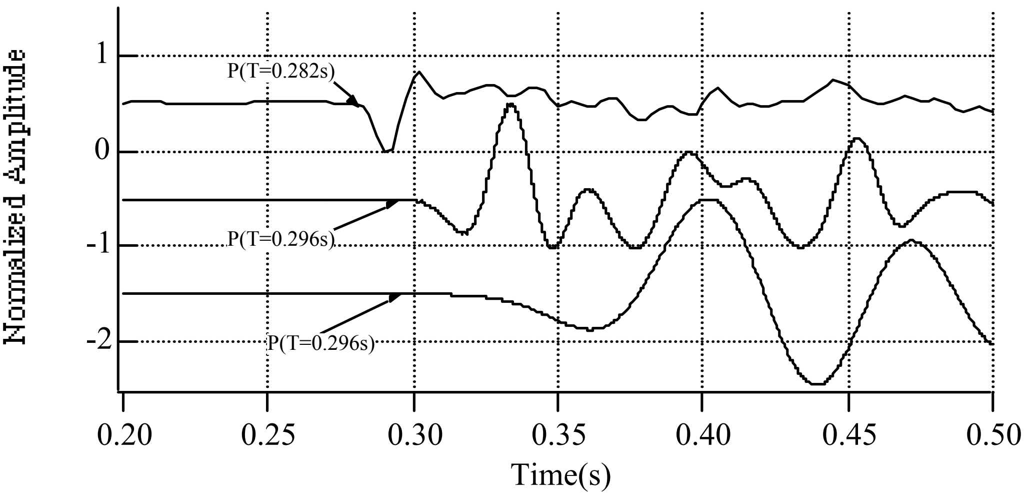

(b)

Fig. 3 Seismograms of 800 m explosion. (a) TA-31, (b) TA-36. Top line shows observed velocity record, middle line shows 2-D and bottom line shows 3-D calculated seismogram in Figs. (a), (b).

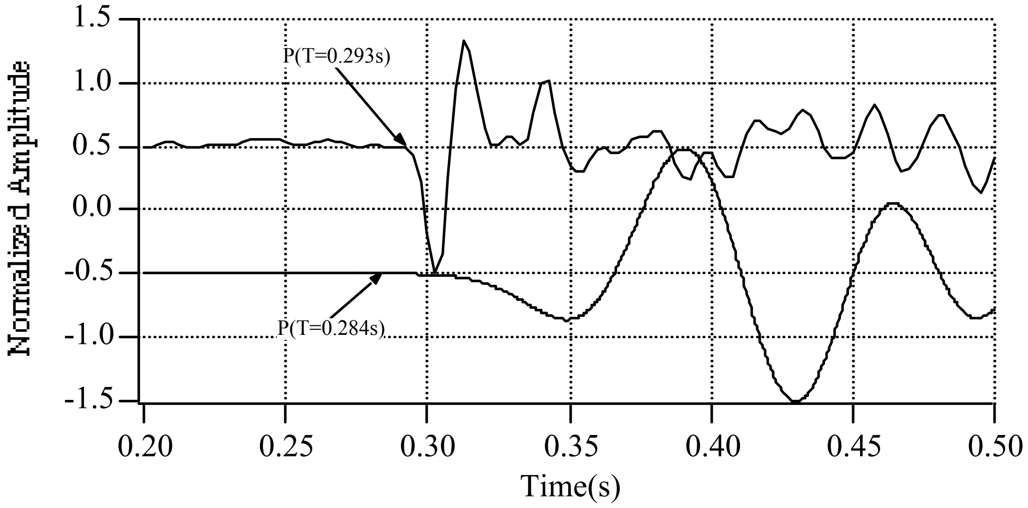

(a)

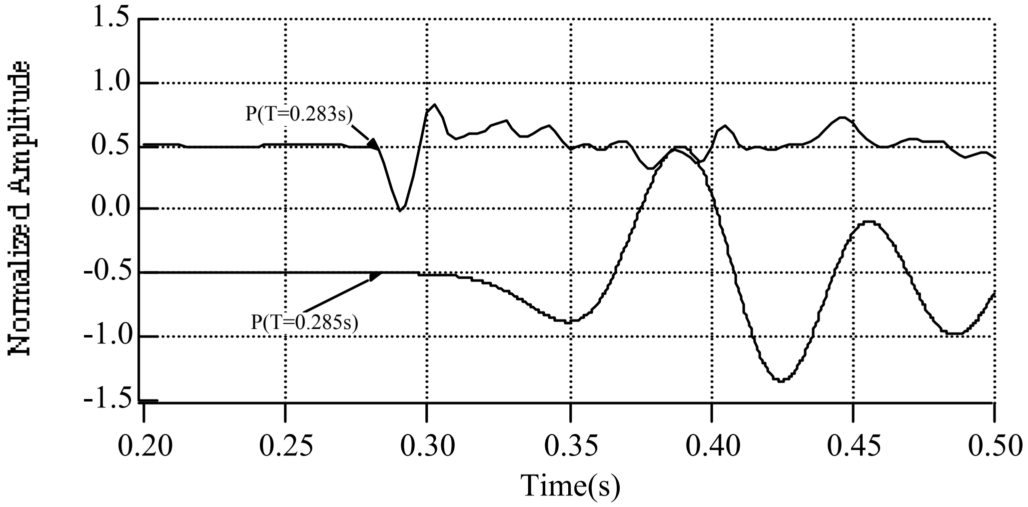

(b)

Fig. 4 Seismograms of 800 m explosion. (a) TA-31, (b) TA-36. Top line shows observed velocity record; bottom line shows 3-D calculated seismogram in Figs. (a), (b).

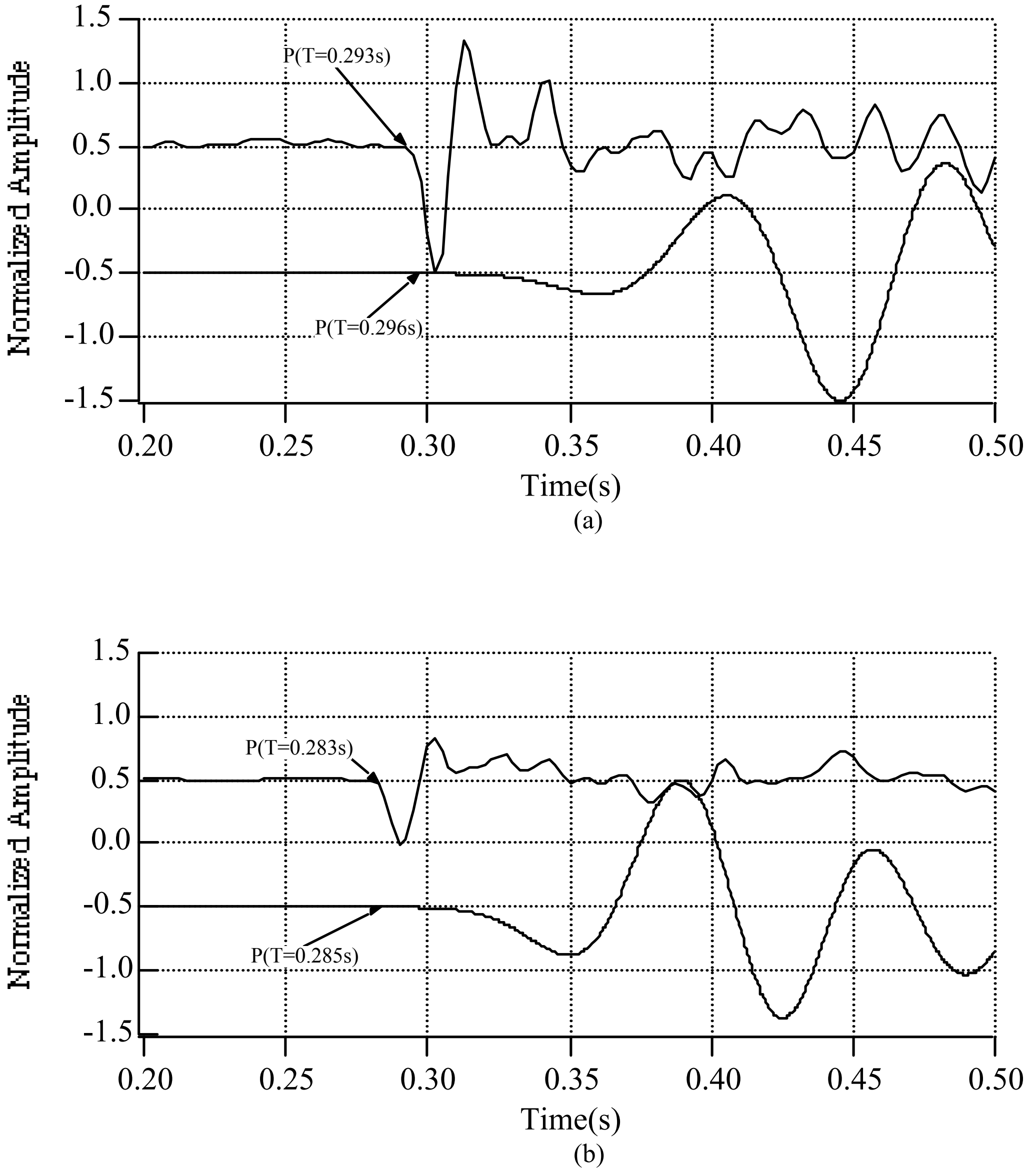

Fig. 5 Seismograms of 800 m explosive. (a) TA-31, (b) TA-36. Top line shows observed velocity record; bottom line shows 3-D calculated seismogram in Figs. (a), (b). This model includes the low velocity zone around TA-31.